

1 **Health burden from food systems is highly unequal across**
2 **income groups**

3 Lianming Zheng^{1,2}, Wulahati Adalibieke^{3,4}, Feng Zhou^{3,4,*}, Pan He^{5,*}, Yilin Chen^{1,2,6}, Peng Guo^{1,2},
4 Jinling He^{1,2}, Yuanzheng Zhang^{3,4}, Peng Xu^{1,2}, Chen Wang^{1,2}, Jianhuai Ye^{1,2}, Lei Zhu^{1,2}, Guofeng Shen³,
5 Tzung-May Fu^{1,2}, Xin Yang^{1,2}, Shunliu Zhao⁷, Amir Hakami⁷, Armistead G. Russell⁸, Shu Tao^{1,2,3,4}, Jing
6 Meng^{9,*}, Huizhong Shen^{1,2,*}

7 ¹Shenzhen Key Laboratory of Precision Measurement and Early Warning Technology for Urban
8 Environmental Health Risks, School of Environmental Science and Engineering, Southern University
9 of Science and Technology, Shenzhen 518055, China

10 ²Guangdong Provincial Observation and Research Station for Coastal Atmosphere and Climate of
11 the Greater Bay Area, Southern University of Science and Technology, Shenzhen 518055, China

12 ³Institute of Carbon Neutrality, Peking University, Beijing 100871, China

13 ⁴Laboratory for Earth Surface Processes, College of Urban and Environmental Sciences, Peking
14 University, Beijing 100871, China

15 ⁵School of Earth and Environmental Sciences, Cardiff University, Cardiff, CF10 3AT, United Kingdom

16 ⁶School of Urban Planning and Design, Peking University, Shenzhen Graduate School, Shenzhen
17 518055, China

18 ⁷Department of Civil and Environmental Engineering, Carleton University, Ottawa, ON K1S 5B6,
19 Canada

20 ⁸School of Civil and Environmental Engineering, Georgia Institute of Technology, Atlanta, Georgia
21 30332, United States

22 ⁹The Bartlett School of Sustainable Construction, University College London, London WC1E 7HB,
23 United Kingdom

24 *Corresponding author, e-mail: zhouf@pku.edu.cn; hep3@cardiff.ac.uk; jing.j.meng@ucl.ac.uk;
25 shenhz@sustech.edu.cn

26

27 **Abstract**

28 Food consumption contributes to the degradation of air quality in regions where food is produced,
29 giving rise to an often-neglected form of environmental inequality, i.e., the contrast between the
30 environmental health burden caused by the food consumption of a specific population and that
31 they encounter as a consequence of food production activities. Herein, we explore this inequality
32 within China's food system, by linking air pollution-related health burden from the production side
33 to the consumption side at high levels of spatial and sectorial granularity. Our findings reveal that
34 low-income groups bear a 70% higher air pollution-related health burden from the food production
35 than is caused by their food consumption, while high-income groups benefit from a 29% lower
36 health burden relative to their food consumption. We show that current interventions such as
37 agricultural management, dietary transition, crop reallocation, and economic policies do not
38 uniformly address both environmental pressure and inequality, emphasizing the need for a
39 combination of measures to establish a sustainable and equitable food system.

40 **Introduction**

41 Agricultural intensification and redistribution have significantly increased food productivity and the
42 abundant and diverse food supply^{1,2}. However, these practices have also resulted in an uneven
43 distribution of the environmental footprint of the food system. Emissions embedded in the food
44 system are spread across various food-producing regions that may be far from where the food is
45 consumed. Globally, 26%–64% of the population cannot fulfill their crop demand solely through
46 crop production within a 1000-km radius³. In China, Henan, Hebei, and Shandong provinces
47 accounted for about one-third of agricultural NH₃ emissions⁴, while local food consumption only
48 constituted 11%–19% of the national food consumption⁵. Consequently, food contributes one of
49 the greatest disparities in consumption-based PM_{2.5} pollution exposure among all goods⁶,
50 potentially leading to significant environmental inequality among different groups of people. In the
51 context of the United States, for example, it has been observed that the per-capita food
52 consumption among Whites/others causes 49–61% higher exposure to air pollution than that
53 among Blacks/Hispanics⁶.

54 In alignment with the United Nations Sustainable Development Goals, the modern food system
55 needs to feed the global population to provide nutritional security with low environmental impact
56 and without contributing to social injustice⁷⁻¹³. To avoid a disproportionate allocation of health

57 outcomes to a small subset of the population, a key step is to explicitly evaluate the inequality of
58 the health damage attributed to the food system, which is rarely discussed. Key factors such as
59 food categories, spatial heterogeneity, and potential drivers (e.g., household wealth) have not
60 been adequately explored, impeding efforts to reduce inequality. Taking food categories as an
61 example, ruminant meat, especially beef, has the highest environmental impact compared to non-
62 ruminant meat, whereas plant-based foods have the least impact^{14,15}. However, the manner and
63 degree to which food categories affect general health-related inequalities remain unknown, and it
64 is unclear whether existing intervention strategies aimed at alleviating environmental burdens and
65 mitigating the negative health effects of the food system can provide co-benefits in reducing
66 related inequalities.

67 Expanding on this concept, we examine the air pollution–related inequality within China’s food
68 system. As the world’s leading agricultural producer, China has experienced significant agricultural
69 intensification due to its large population and relatively limited per-capita arable land area
70 compared to the global average¹⁶. These factors and a diverse dietary transition¹⁷ make China’s
71 food system an important case for understanding air pollution–related inequality.

72 **Results**

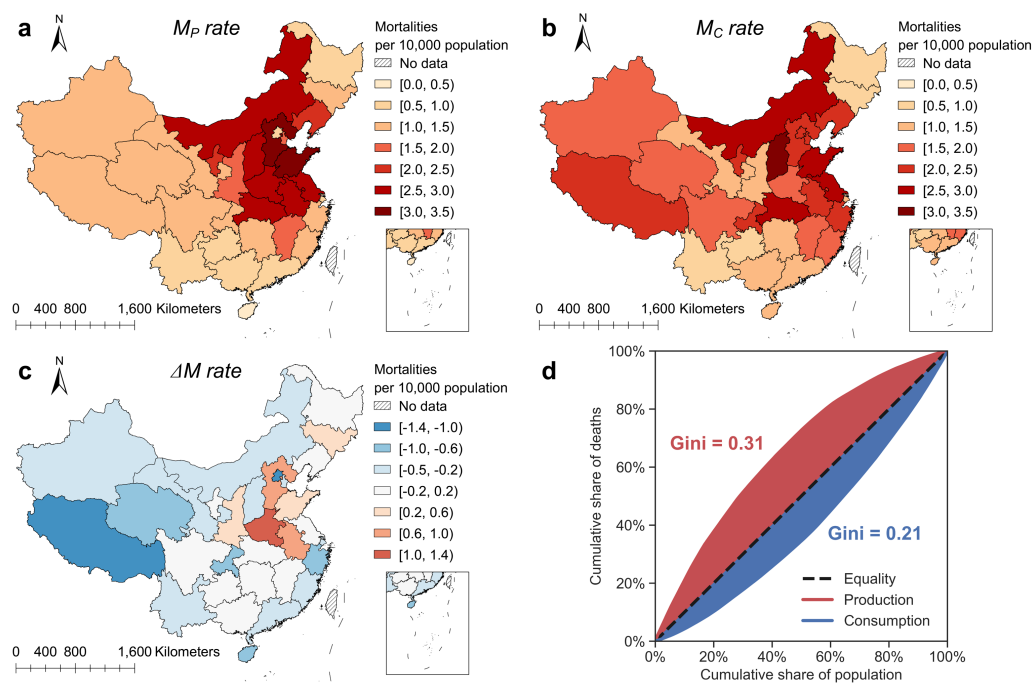
73 **Spatial heterogeneity in air pollution–related health impact**

74 We quantified air pollution–related health damage, represented by premature mortality,
75 throughout the food supply chain. Our analytical framework integrates several components: a
76 high-resolution emission inventory (1 km × 1 km for cropland ammonia emissions and livestock
77 management, 10 km × 10 km for all other sectors); a provincial-level input–output table; and an
78 advanced backward sensitivity analysis technique implemented within a regional chemical
79 transport model (CMAQ-Adjoint)¹⁸. Using the adjoint model enabled us to trace air pollution–
80 related health damage from production to consumption across nine distinct food categories at a
81 high level of spatial and sectoral granularity (Methods and Data). This finer resolution surpasses
82 previous studies and enables the investigation of air pollution–related inequality within the food
83 system.

84 In general, the food system in China was responsible for approximately 0.26 million premature
85 deaths related to ambient PM_{2.5} exposure in 2017. Most (74%) of these deaths are attributed to
86 NH₃ emissions, an important precursor of ambient PM_{2.5}, during food production, such as crop

87 cultivation and livestock breeding. The remainder (26%) are caused by emissions of primary PM
 88 and other precursors, including SO₂ from power plants and NO_x from motor vehicles, during the
 89 distribution, aggregation, processing, packaging, and marketing of food products. This food-
 90 induced air pollution-related mortality represents 12% of overall annual mortality from exposure
 91 to ambient PM_{2.5} in China. Of this mortality, meat contributes 55%; grain contributes 30%; and
 92 vegetables, fruits, and nonmeat animal products (including eggs and dairy) account for the
 93 remaining 15% (see Supplementary Text S1 for a comparative analysis of our results and previous
 94 studies).
 95 Northern and Eastern China are the regions most affected by food production (Figs. 1a and S1),
 96 and 41% of the mortality is attributable to food production (defined as “ M_P ”) concentrated in
 97 Shandong, Henan, Hebei, and Jiangsu (Fig. S1). The Gini coefficient, representing the inequality of
 98 spatial disparity for M_P , is estimated to be 0.31 on average and ranges from 0.30 to 0.64 by food
 99 type (Fig. 1d and Fig. S2).

100



101

102 **Fig. 1 | Provincial-level distributions and inequalities of premature mortalities due to food**
 103 **production and consumption in China.** Annual premature mortality rates from (a) food production
 104 (M_P rates) and (b) food consumption (M_C rates). (c) Difference between M_P rates and M_C rates (ΔM
 105 rate). (d) The Gini coefficients of M_P rates and M_C rates. The provincial boundary shapefile is

106 sourced from <https://www.resdc.cn/DOI/DOI.aspx?DOIID=122>.

107

108 The distribution of premature mortality rates based on food consumption (“ M_C ” rates) is more
109 dispersed than that of M_P rates (Fig. 1b). The largest provinces associated with per-capita food
110 consumption and the highest air pollution–related mortalities are Shanxi, Inner Mongolia,
111 Shandong, Hubei, and Jiangsu. Two categories of regions emerged. The first category pertains to
112 highly developed regions with wealthy populations, such as Beijing, Shanghai, Zhejiang, and
113 Guangdong, which show higher M_C rates than the others. The second category represents
114 concentrated food-producing regions with developed agricultural production, such as Henan and
115 Hebei, where M_C are far below M_P . The spatial inequality of M_C is significantly lower than that of
116 M_P , with a Gini coefficient of 0.21 on average (ranging from 0.23 to 0.53 across different food types;
117 Fig. 1d and Fig. S2). The low inequality of M_C is attributed to a convergence toward a modernized
118 diet characterized by high meat consumption in the last few decades⁵, which is consistent with
119 global patterns^{19,20}.

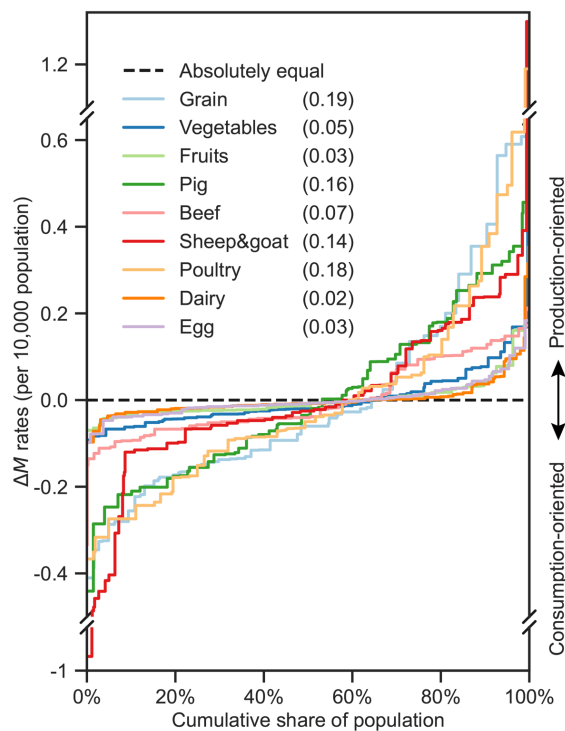
120 **Inequality by food categories**

121 We calculated the difference between M_P and M_C rates, presented as ΔM rate in Fig. 1c (Methods
122 and Data). Positive ΔM rates indicate that people in the region face a larger health burden from
123 food production than that caused by food consumption (“production-oriented”), whereas negative
124 ΔM rates signify the opposite (“consumption-oriented”). Overall, the ΔM rates vary geographically
125 across the country. The consumption-oriented provinces include (1) regions with poor crop-
126 growing conditions (e.g., Qinghai and Tibet) that face constraints with regard to food production
127 and (2) highly developed regions (including provincial-level municipalities, such as Chongqing and
128 Beijing, and coastal provinces, such as Zhejiang) where the industrial focus has shifted from
129 agriculture to other industries²¹. Notably, the results of ΔM rates are strongly influenced by
130 population size, as the considerably difference between the M_P and M_C rates in the total mortality
131 would be scaled down owing to the high population in per-capita terms (e.g., Guangdong, as shown
132 in Fig. S1) and vice versa (e.g., Tibet, Hainan, and Qinghai).

133 Henan exhibited the highest positive ΔM rate, with 1.06 premature deaths per 10,000 population.

134 This region experiences severe food-induced air pollution, which locally causes 2.95 premature
135 deaths per 10,000 population. Comparatively, food consumption in Henan is responsible for 1.88

136 premature deaths per 10,000 population nationwide. Thus, the population in Henan bears a 57%
 137 higher health burden due to food production than that caused by their food consumption.
 138 Conversely, Beijing exhibited the lowest ΔM rate, with a value of -1.32 (0.74 and 2.06 for the M_P
 139 and M_C rates, respectively, and a 64% lower health burden). Because the Gini coefficient does not
 140 apply to the ΔM rate with positive and negative values, we developed a Supply–Demand Health
 141 Inequality Index (SDHII) to estimate national inequality in the ΔM rates. This index was employed
 142 to evaluate the national degree of health inequality compared with an ideal state of complete
 143 equality (Methods and Data; Fig. S3) and to ensure the comparability of the inequality between
 144 specific sectors and food categories.
 145



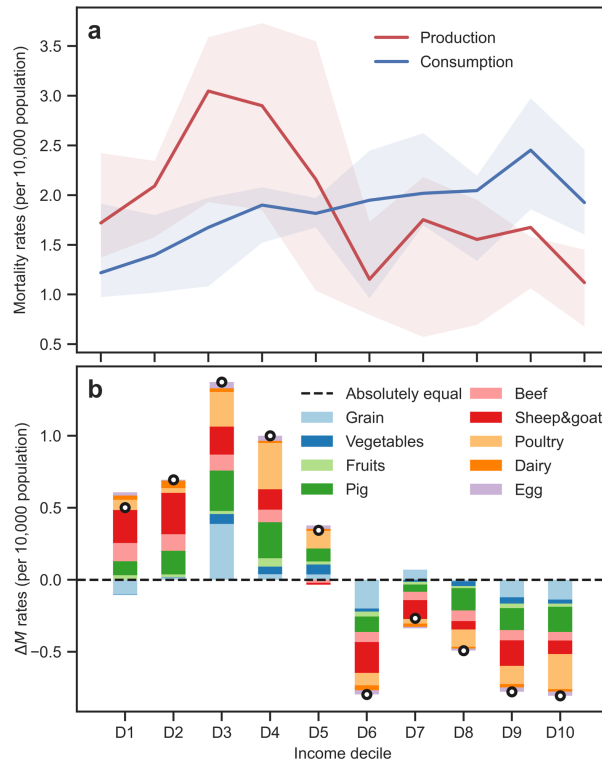
146
 147 **Fig. 2 | Inequality within the food system across food types.** Shown are ΔM rates (difference in
 148 mortality rates attributable to $PM_{2.5}$ exposure from food production versus consumption) of each
 149 province, sorted in ascending order. The provinces with ΔM mortality rates >0 (on the right side of
 150 the curves) are “production-oriented” provinces, indicating that the mortality from local food
 151 production surpass that attributed to food consumption. Conversely, if the ΔM rates are <0 (i.e.,
 152 “consumption-oriented” provinces), the opposite holds true. The inequalities are quantified as the
 153 Supply–Demand Health Inequality Index, indicated in parentheses in the legend for each food type.
 154

155 Grain, poultry, and pig were identified as the top three food types associated with the highest
156 inequality, whereas vegetables, fruits, and nonmeat animal-sourced foods (eggs and dairy)
157 demonstrated minor inequality (Fig. 2 and Table S1). The low level of inequality associated with
158 vegetables and fruits can be attributed to their smaller environmental footprint, perishable nature,
159 and difficulties in storage²². When considering inequality across protein types, the disparity is
160 considerably greater for animal-sourced protein than for plant-sourced protein, particularly for red
161 meat and poultry (Fig. S4). In highly developed and coastal provinces, the health cost of producing
162 1 kg of protein was significantly higher than the cost of consuming 1 kg of protein (e.g., 2–9 times
163 higher in Beijing, Shanghai, and Tianjin compared with the current consumption cost; Fig. S4, right
164 end of the curves).

165 We investigated the inequality of the food system between rural and urban areas at different
166 income levels. Pronounced gaps in ΔM rates exist between rural and urban areas (Fig. S5) due to
167 the rural-urban differences in M_p and M_c rates (Fig. S6). Depending on food type, 57%–94% of the
168 rural population is exposed to higher health risks from production (Table S2) than they should be
169 according to their consumption, compared to only 0%–22% for their urban counterparts.
170 Particularly for red meat, over 90% of the rural population bears an excess health burden,
171 compared to 0%–16% for the urban population.

172 M_c rates increase with income (Fig. 3a). The highest mortality rate occurred in the second highest
173 income group, D9 (2.45 deaths per 10,000 population). However, a significant decline was
174 observed in the top income group, D10 (1.43 deaths per 10,000 population; Fig. 3a). This decline
175 is attributed to the lowest contribution of meat consumption to per-capita deaths in D10 compared
176 to other high-income groups (D6–D9), suggesting that the highest income group is more health-
177 conscious and consumes a more appropriate amount of meat. In contrast, M_p are generally
178 negatively correlated with income, although the lowest income groups (D1–D2) do not follow this
179 trend due to harsh local conditions for crop growth (e.g., rural areas in Gansu, Qinghai, and Tibet).
180 Overall, low-income groups (D1–D5) experienced 70% more health damage than high-income
181 groups (D6–D10), but food consumption in the former caused 29% less health damage, leading to
182 positive ΔM rates among low-income groups, negative ΔM rates among high-income groups, and
183 net inequality over income, which is dominated by animal-based food (Fig. 3b). The ΔM rate of D6
184 is as low as that of the highest income groups D9–D10, mainly because these groups comprise

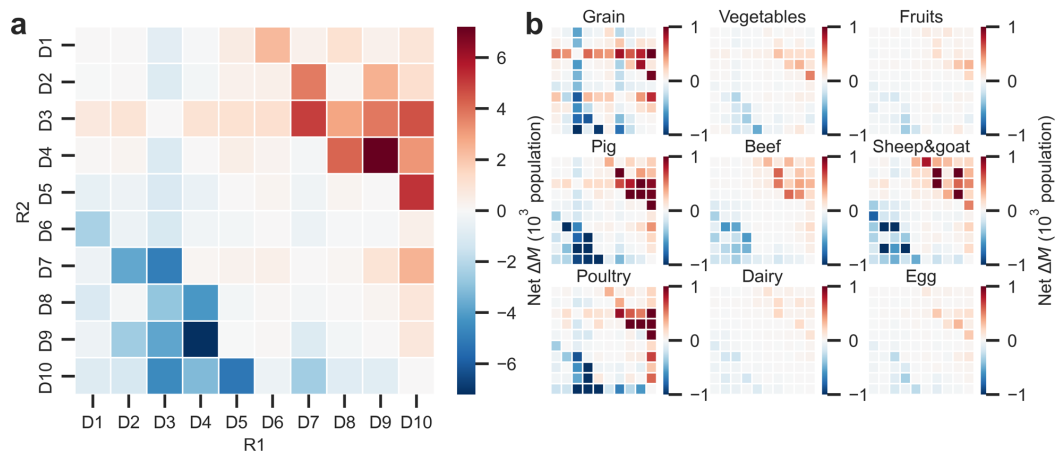
185 urban areas in provinces with poor planting conditions (e.g., urban areas in Qinghai and Shanxi),
 186 resulting in the lowest M_p rate from grain among all income groups.
 187



188
 189 **Fig. 3 | Mortality disparity across income groups. (a)** Relationship between income and premature
 190 mortality, including premature mortality rates attributed to food production (M_p rates) and
 191 consumption (M_c rates). The shading indicates the range between the 25th and 75th percentiles.
 192 **(b)** Mortality rate differences attributable to $PM_{2.5}$ exposure from food production vs. consumption
 193 (ΔM per 10,000 population) by income decile. The impacts of various food types on ΔM rates differ
 194 among income groups, with each type contributing positively or negatively. The net ΔM rates are
 195 presented as black dots.

196
 197 To trace the sources of inequality caused by food supply between income groups, we calculated
 198 net ΔM by deducting the portion that achieved a balance between mutual trade across specified
 199 income groups (Methods and Data). The connection between income and net ΔM was evident (Fig.
 200 4a). Generally, higher income groups (D6–D10) exhibit fewer net ΔM because of their limited food
 201 exports to lower income groups (D1–D5), whereas the lower income groups bear greater health
 202 damage from supplying food to higher income groups. Notably, D3–D5 suffered more from food

203 supply (positive net ΔM) than the D7–D10 groups (Fig. 4a, upper right), while net less health cost
 204 (negative net ΔM) is observed in D7–D10 (Fig. 4a, lower left). Similar results were observed across
 205 all food types (Fig. 4b), indicating that high-income groups transfer the environmental externalities
 206 through interregional food trades, while low-income groups bear excess health damage, regardless
 207 of food type. By comparing premature mortalities resulting from self-production and consumption
 208 and interregional food trade, we found that the proportion of self-production and consumption
 209 increased with income (Fig. S7 and S8). This suggests that agricultural products in developed
 210 regions are primarily produced to meet local demand rather than being traded on the national
 211 market for revenue. Considering all end-use sectors, we found that food contributes 41.7% of the
 212 total inequality of all end-uses in China (Fig. S9 and Table S3), being the largest among all goods
 213 and services.
 214



215
 216 **Fig. 4| Mortality tracing between income groups.** Each cell represents the gap of premature
 217 mortality after deducting the equivalent mortality due to mutual food supply between two given
 218 income groups (defined as “net ΔM ”). Each group serves as the food supplier for the other group.
 219 This result represents the difference in mortality between the two designated regions after
 220 accounting for their production–consumption tradeoff. As each region is simultaneously a source
 221 and receptor, we defined “R1” and “R2” to establish the direction for statistical and visual purposes.
 222 If the number of deaths is positive, the group in “R1” caused a net ΔM toll suffered by “R2,” while
 223 negative means the opposite. For instance, the positive result in the cell at the intersection of the
 224 D4 row and D9 column indicates that more health damage is incurred on D4 by D9 in mutual supply.
 225 We analyzed each type of food **(b)** and then aggregated the results for all foods to obtain the overall

226 outcome (a).

227

228 **The potential of intervention strategies to improve equality**

229 We conducted a series of simulations to explore whether current efficient interventions aimed at
230 reducing environmental pressure and health damage could lead to co-benefits in reducing
231 inequality. These strategies can be classified as emission mitigation, diet transition, and food
232 production reallocation, each incorporating implementations of varying intensity (Table S4).

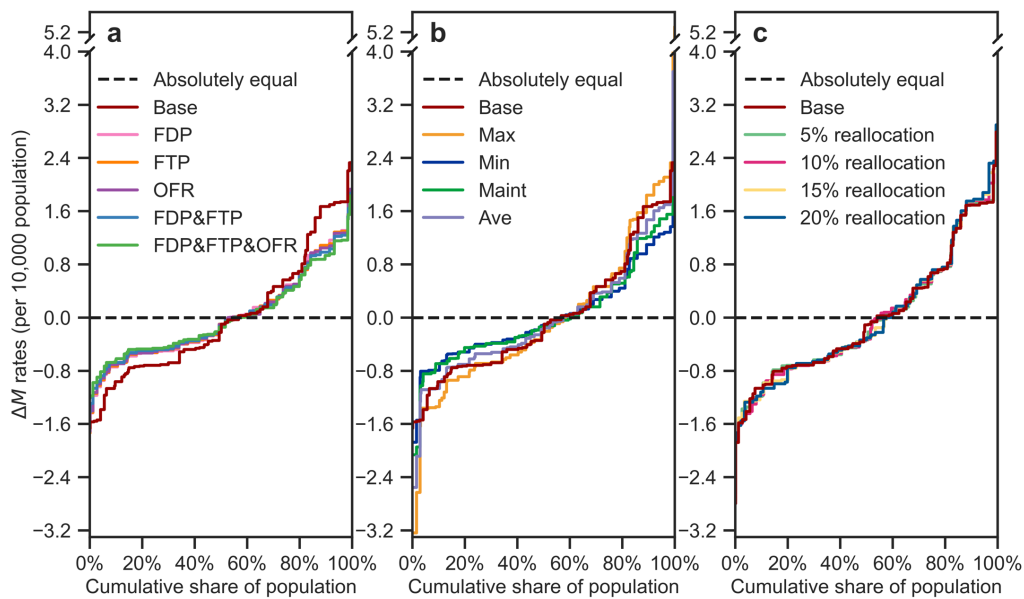
233 Production-based emission mitigation scenarios lead to a noticeable improvement in inequality,
234 reducing it by 26–35% in SDHI across all mitigation strategies (Fig. 5a). These strategies also result
235 in a more balanced distribution of the population that experiences more or less health damage
236 (Table S5). The reduction in inequality among all production-based mitigation interventions
237 primarily stems from decreased inequality within grain production (Fig. S10).

238 The effect of diet transition approaches exhibits considerable variability (ranging from –18% to 30%
239 reduction; Fig. 5b), even with moderate scenarios, e.g., minimal adjustments of the current diet
240 toward the recommended range, referred to as “Maint,” and consuming the average of the
241 recommended range, referred to as “Ave.” The “Maint” scenario demonstrates a 30% decrease in
242 inequality, whereas the “Ave” scenario exhibits a limited effect (6% reduction). This implies that
243 the former is the most favorable dietary option, as it is the most practical choice for policy
244 measures involving the minimal required transition in diets. The key reason for the limited
245 effectiveness of certain dietary transition schemes (e.g., maximal adjustment to the current diet,
246 referred to as “Max”) is that while reducing meat consumption contributes the most to improving
247 equality, the benefits are offset by consuming plant-based foods (such as grain, vegetables, and
248 fruits) and nonmeat animal-based foods (including dairy and eggs; Fig. S11). Moreover, diet
249 transition scenarios exhibit limited effectiveness in reducing the unequal distribution of the
250 population affected by disproportionate health damage, regardless of considering the details in
251 several subscenarios (Table S5).

252 For the food production reallocation scenarios, although the mortality rate decreases with
253 increasing reallocation levels (Fig. S12), inequality increases slightly (Table S5 and Fig. 5c),
254 suggesting that agricultural reallocation aimed at reducing health damage is insufficient for
255 alleviating inequality. Nevertheless, a slightly more equitable distribution among population

256 groups with varying levels of health damage was observed (Table S5).

257



258

259 **Fig. 5 | The changes in the food system inequality in response to different intervention strategies.**

260 These strategies include (a) emission mitigation, (b) diet transition, and (c) food reallocation. Each
261 scenario includes specific subscenarios to reflect the impacts of different intervention intensities
262 on inequality. For food reallocation, we conducted 20 subscenarios ranging from 1% to 20%
263 reallocation of total food production and found no significant change in the distribution curve. To
264 provide clarity, we provide four subscenarios (5%, 10%, 15%, and 20% reallocation) and the base
265 case (0% reallocation) for comparison.

266

267 In addition to supply and demand-side interventions, economic policies such as taxation and
268 subsidies can complement efforts to reduce inequality. By evaluating the value of a statistical life,
269 we quantified the appropriate food tax that should be implemented or subsidy that should be
270 provided in each region (Fig. S13) and income group (Fig. S14). Our findings indicate that middle-
271 to high-income groups (D6–D10) should be subject to a 4%–14% food tax to compensate for the
272 excess damage suffered by low- to middle-income groups (D1–D5), which could cover 6%–138% of
273 the latter’s food costs.

274 Discussion

275 Revealing the inequalities of health damage within the food system is crucial for understanding
276 environmental justice and achieving the United Nations Sustainable Development Goal of reducing

277 inequalities²³. Our findings contribute to the ongoing discussion about the health effects of food
278 systems, focusing on the equality of air-related health impacts. By linking food production and
279 consumption, we highlight the disparities and inequalities between supply and demand ends
280 across space and food types. Our findings uncover significant and disproportionate differences in
281 air pollution–related health damage per-capita. Higher geographical inequality in production than
282 consumption is observed, perhaps due to increasing agricultural intensification and resulting
283 differences in provincial agricultural emissions. Another possible reason for the smaller demand-
284 side inequality is the convergence toward regional diets over time, possibly due to the Chinese
285 government’s efforts to promote and guide healthy diets and improve living standards²⁴.

286 Our work provides a spatially resolved, food-specific analysis of health-effect inequalities within
287 the food system. We identified optimal schemes to simultaneously reduce health damage and
288 associated inequality, expanding the options available for developing and implementing dedicated
289 mitigation policies. Nevertheless, substantial obstacles and challenges need to be addressed. For
290 example, a trend of mortality may not consistently align with that of equality when adopting
291 certain more sustainable interventions, particularly on a regional scale (e.g., the regions indicated
292 at both ends of the curve in Fig. 5c and Fig. S12). With the expected increase in agricultural
293 intensification, concentrating food production in certain regions could widen the differential
294 burdens of negative externalities of food production among regions and populations. Identifying
295 the leverage points that balance agricultural yield, emission reduction, and equitable distribution
296 of pollution burdens presents a complex problem for policymakers. Furthermore, implementing
297 diversified regulations and protocols to reduce inequality can be challenging. Our results show that
298 food consumption recommendations (e.g., self-production and marketing, or import from other
299 regions; food intake) may need to vary based on regional specifics, which could hinder the
300 development and adoption of policy-related measures, especially when coordination between
301 national and local policies is critical. Given the intricacy of food system transformation,
302 policymakers must concurrently develop short- and long-term policies to address future challenges.
303 In the short term, achieving a more equitable distribution of negative externalities in the food
304 system may not be immediately feasible, so economic measures are recommended to compensate
305 for excess health damage, such as implementing food taxes to subsidize food production regions
306 (Fig. S13 and Fig. S14). In the long term, policymakers need to phase in top-level design and

307 restrictive policies for food system emissions and the related equality, accounting for factors such
308 as the spatial heterogeneity of health costs associated with food production, anticipated dietary
309 transitions in the local context, and nutritional requirements due to population growth, as well as
310 the overall sustainability goals pursued by the nation. Our research explores the potential synergies
311 between health damage and inequalities (Fig. 5), thus providing a solid scientific foundation for
312 effectively formulating such policies.

313 As the world's most populous country, China faces tremendous pressure on its food supply system
314 due to improved living standards. While the development of agricultural intensification and mature
315 food supply chains has satisfied the food demands, they have also led to significant food system-
316 related inequalities. It is worth noting that China is not alone in experiencing these inequalities. In
317 a follow-up first-order analysis that expands the current assessment scale, we found that countries
318 worldwide, particularly middle- and high-income countries, exhibit significant inequality in
319 agricultural ammonia emissions exposure (Supplementary Text S2, Fig. S15). This observation
320 indicates that countries with more advanced food systems may encounter greater challenges
321 relating to agricultural emissions and associated inequalities. Our study illuminates the issue of
322 food system inequality, offers valuable guidance for policymakers in China while also serves as a
323 point of reference for the sustainable development of food systems worldwide.

324 **Methods and Data**

325 We developed a comprehensive modeling framework to estimate the health damage due to PM_{2.5}
326 pollution exposure from the food system in China and analyzed the associated health damage
327 inequality (Fig. S16). The development of the framework includes several steps. Initially, the
328 atmospheric emissions from the supply and demand sides of the food system were linked using
329 the Multi-Regional Input–Output (MRIO) model²⁵. Then, we used the Global Exposure Mortality
330 Model (GEMM)²⁶ to estimate premature mortality associated with ambient PM_{2.5} exposure and
331 the sensitivities of premature mortality to ambient PM_{2.5} concentrations by grid cell. Subsequently,
332 we coupled the concentration sensitivities into multiphase Adjoint for the Community Multiscale
333 Air Quality (CMAQ-Adjoint) model¹⁸ to compute the sensitivities of premature mortality to
334 emissions. These matrices encompass all pollutant species, locations, and time, allowing us to
335 estimate their relative contributions on both the supply and demand sides. To analyze inequality,
336 we developed a new index, SDHII, to quantify the national inequality pattern in the gap between

337 PM_{2.5}-related premature mortality associated with food supply and demand. The detailed
338 procedures are described in the following sections.

339 **Linking atmospheric emissions from food production to consumption**

340 We initiated our study by developing a production-based emission inventory of all the production
341 sectors of China in 2017, for which the global high-resolution emission inventory product (10 × 10
342 km) published by Peking University (PKU-Inventory) for atmospheric emissions across sectors (e.g.,
343 power generation, industry, transportation, and agriculture) and fuel types (e.g., coal, oil, natural
344 gas, and biomass) was used²⁷. Additionally, a Chinese agricultural emission inventory with 1 × 1 km
345 resolution developed by Adalibieke et al.²⁸ (crop ammonia volatilization) and Wang et al.²⁹
346 (livestock management) was employed to calculate the emissions associated with agricultural
347 activities. This comprehensive inventory covered ammonia emissions from the production of nine
348 food categories, including grain, vegetables, fruits, pig, beef, sheep and goat, poultry, dairy, and
349 eggs. The emissions from dairy and egg products considered in this study arise from the rearing
350 processes of dairy cows and egg-laying hens. By integrating this food emission inventory into the
351 PKU-Inventory, we expanded the current inventory to provide a detailed account of agricultural
352 emissions. Subsequently, we reallocated all the atmospheric pollutants according to provinces to
353 align them with the production sectors in the MRIO models using Energy Balance Sheets from the
354 China Energy Statistical Yearbook³⁰. The resulting provincial production-based emission inventory
355 comprised 42 production sectors corresponding to the MRIO production sectors of the nine food
356 categories.

357 To establish a link between pollutant emissions between the food supply and demand sides, we
358 employed Environmental Extended Input–Output Analysis (EEIOA) to create a consumption-based
359 emission inventory. EEIOA is an extended application of input–output analysis that enables the
360 explicit analysis of environmental impacts³¹. Initially, we employed traditional economic
361 accounting, expressing the input–output link function as Eq. (1):

$$362 \quad X = (I - A)^{-1}Y \quad (1),$$

363 where X represents the economic output matrix, A is a normalized matrix of intermediate
364 coefficients where columns correspond to the input required from sectors in a given region to
365 produce one unit of the output of each sector in another region, $(I - A)^{-1}$ is the Leontief inverse
366 matrix, and Y is a vector of the finished consumption. Subsequently, we incorporated emission

367 information using Eq. (2):

$$368 \quad E = f(I - A)^{-1}Y \quad (2),$$

369 where E represents atmospheric emissions embedded in flows of goods and services between the
370 sectors. The matrix f is diagonal, with emission intensities (emissions for unit output) for each
371 sector along the diagonal and zeros in all the other positions.

372 A consumption-based emission inventory (referred to as S) was generated using EEIOA that
373 illustrates how emissions are embodied in the flows of goods and services among the production
374 sectors, ultimately reaching the final consumption sectors. This inventory includes 31 provincial-
375 level administrative divisions (excluding Taiwan, Hong Kong, and Macao, as data for these regions
376 were unavailable), 42 production sectors, and 5 consumption sectors.

377 The consumption-based emission inventory quantifies virtual emission flows specific to each
378 region, spanning from supply to demand sides. Subsequently, we calculated the emissions
379 attributed to production (E_p) and consumption (E_c) at the provincial level using Eq. (3) and (4):

$$380 \quad E_p = \sum_c S \quad (3)$$

$$381 \quad E_c = \sum_p S \quad (4),$$

382 where S represents the consumption-based inventory; p and c is the supply and demand sides of
383 the inventory, respectively; E_p is a transposed matrix of $(E_p^1 \ E_p^2 \ E_p^3 \ \dots \ E_p^Q)$, where E_p^i
384 represents the production-based emissions in a given province i , and Q is the total number of
385 administrative divisions (31 in this study, excluding Hong Kong, Macao, and Taiwan due to data
386 limitations). Similarly, E_c is a transposed matrix of $(E_c^1 \ E_c^2 \ E_c^3 \ \dots \ E_c^Q)$, where E_c^i denotes
387 the consumption-based emissions in a given province i .

388 Next, we computed the relative contribution of emissions for each province at both the supply and
389 demand ends, denoted as:

$$390 \quad r_{i,j} = \frac{S_{i,j}}{\sum_{c=1}^Q S_{i,c}} \quad (5),$$

391 where $r_{i,j}$ represents the relative share of emissions within a given region i at the supply side,
392 concerning region j at the consumption end. To consolidate all relative shares of emissions along
393 the supply chain, we employed the matrix R , defined as:

$$394 \quad R = \begin{pmatrix} r_{1,1} & \dots & r_{1,Q} \\ \vdots & \ddots & \vdots \\ r_{Q,1} & \dots & r_{Q,Q} \end{pmatrix} \quad (6),$$

395 where R incorporates all the relative shares of emissions.

396 To appropriately allocate agricultural emissions within the food supply chain, we applied a double
397 constraint to this portion of the emissions. First, we extracted the economic flow from the
398 agricultural sectors to the rural and urban consumption sectors, as generated by the MRIO model.
399 Next, we redistributed the food emissions of each province by (1) calculating the relative share of
400 monetary flows from each province on the demand side to provinces on the demand side, yielding
401 a supply-side constraint matrix (labeled as H_1); (2) determining the total amount of annual per-
402 capita food consumption in 2017 for each food type using data from the Chinese National Bureau
403 of Statistics⁵; and (3) matching the total food consumption to that of each province in the demand
404 side and redistributing it according to H_1 . These steps ensured that the relative proportions of each
405 food type in the supply side for a given province were adequately constrained. Each food type was
406 individually distributed on the demand side based on the scaling factors.

407 To ensure that the total amount of emissions was conserved for each food type from the supply to
408 demand side, we calculated the relative share of the amount of food in the aforementioned result
409 for each province on the supply side as an emission-constraint matrix (labeled as H_2). Subsequently,
410 we redistributed agricultural emissions from the supply side to the demand side using H_2 . Notably,
411 we did not conduct a detailed analysis of the residential sectors because the overall estimation
412 framework is based on the reclassification of the production sectors. Nevertheless, we treated this
413 part as a whole and accounted for it when evaluating the contribution of each component to the
414 premature mortality³².

415 **Health damage estimation**

416 The latest version of the CMAQ-Adjoint, version 5.0, was utilized in our study to quantify the
417 contributions of location-, time-, and pollutant-specific emissions to premature mortality. CMAQ-
418 Adjoint is comprised of two models: a forward model, which mirrors the original CMAQ base model,
419 and a backward model. We applied CMAQ-Adjoint to a geographical domain encompassing East
420 Asia, defined by 124×184 horizontal grid cells at a resolution of 36 km, and 13 vertical layers
421 extending to approximately 16 km above ground. For evaluation, a 1-year simulation using the
422 CMAQ base model was conducted. The results have been illustrated in a previous study, indicating
423 a general concordance with observed spatial distributions and temporal trends of multiple
424 pollutants.

425 The backward model allowed us to calculate sensitivities, that is, the partial derivatives of the
 426 objective function concerning related input parameters. By defining the objective function J as the
 427 total premature mortality from ambient PM_{2.5} exposure within China in 2017, we incorporated the
 428 GEMM into the adjoint analysis. The objective function J was expressed by the following equations,

$$429 \quad J = \sum M_{0,x,y} P_{x,y} [1 - e^{-\theta T(z_{x,y})}] \quad (7)$$

$$430 \quad T(z_{x,y}) = \frac{\log(1 + \frac{z_{x,y}}{\alpha})}{1 + e^{-\frac{z_{x,y} - \mu}{\nu}}} \quad (8)$$

$$431 \quad z_{x,y} = \max(0, C_{x,y} - cf) \quad (9)$$

432 where (x, y) denotes a specific model grid cell; $M_{0,x,y}$ represents the baseline mortality rate at grid
 433 cell (x, y) ; $P_{x,y}$ represents the population within grid cell (x, y) ; $C_{x,y}$ denotes the location-specific
 434 annual PM_{2.5} concentration at grid cell (x, y) , in $\mu\text{g}\cdot\text{m}^{-3}$; cf is the concentration threshold below
 435 which no health association is assumed to be identifiable. The term $1 - e^{-\theta T(z)}$ is the GEMM
 436 equation to calculate the population-attributable fraction (PAF)²⁶. As suggested by Burnett et al.²⁶,
 437 the following values for the GEMM parameters were used to calculate PAF of noncommunicable
 438 diseases and lower respiratory infections (NCD+LRI) mortality from ambient PM_{2.5} exposure for
 439 adults aged 25–99: $\theta = 0.1430$, $\alpha = 1.6$, $\mu = 15.5$, $\nu = 36.8$, $cf = 2.4 \mu\text{g}\cdot\text{m}^{-3}$. $M_{(x,y)}$ is determined by the
 440 baseline mortality rate of NCDs+LRIs of the province where (x, y) is located³³. Further details
 441 regarding the parameter configuration of GEMM can be found elsewhere²⁶.

442 We then derived the adjoint forcing term using Eq. (10),

$$443 \quad \varphi_{x,y} = \frac{\partial J}{\partial c_{x,y}} = M_{0,x,y} P_{x,y} \theta e^{-\theta T(z_{x,y})} T'(z_{x,y}) \frac{dz_{x,y}}{dc_{x,y}} \quad (10)$$

444 where $\varphi_{x,y}$ is the adjoint forcing at grid cell (x, y) ; $c_{x,y}$ denotes the PM_{2.5} concentration at grid cell
 445 (x, y) at any time step; $dz_{x,y}/dc_{x,y}$ is equal to the reciprocal of the number of model time steps in a
 446 year and is set to 1/43800 in our simulation (12 minutes per time step); $T'(z_{x,y})$ is the derivative of
 447 $T(z)$ at $z = z_{x,y}$. In the adjoint simulation, these forcing terms were applied to all modeled PM_{2.5}
 448 species as inputs to derive the adjoint sensitivities of mortality to location- and time-specific
 449 emissions of primary PM_{2.5} and precursors. Similar assessment has been conducted in our CMAQ-
 450 adjoint development paper¹⁸. It should be noted that the computational expense of running the
 451 CMAQ-Adjoint model is about fourteenfold compared to the base CMAQ model. A single-day
 452 simulation using the CMAQ-Adjoint model, encompassing both forward and backward simulations
 453 in our study domain, on average necessitates 2.2×10^5 seconds of CPU time. Extrapolating this to

454 the one-year timeframe of our study, the cumulative CPU time approximates 8.2×10^7 seconds,
455 translating to roughly 950 days.

456 We extracted the premature mortalities from the production sectors related to the food system
457 using the adjoint sensitivities. The premature mortalities specified by production sectors were then
458 linked to the consumption sectors of both rural and urban residents based on the input-output
459 analysis. This process yielded a dataset of PM_{2.5}-related health damage for the entire food system,
460 facilitating further analysis of inequality. In contrast to previous methods that directly calculate
461 sector and species contributions using the objective function in the production or emission
462 sector³⁴⁻³⁶, our approach establishes a connection between mortality, production, and
463 consumption sectors within the food system based on the consumption-based emission inventory.

464 **Inequality evaluation in premature mortality related to PM_{2.5} exposure**

465 We introduced the novel SDHII to evaluate the national inequality between PM_{2.5}-related health
466 damage attributed to the food supply and demand sides. The calculation process comprises two
467 steps.

468 First, we calculated the disparity between premature mortalities attributed to food production (M_P)
469 and consumption (M_C) for each province, which is denoted as ΔM^i and represents the difference
470 in health damage incurred in a region owing to local food production versus the health damage
471 expected from local food consumption within the same region (accounting for local and nonlocal
472 food sources). Mathematically, it is defined by Eq. (11):

$$473 \quad \Delta M^i = M_P^i - M_C^i \quad (11),$$

474 where M_P^i and M_C^i represent the M_P rate (deaths per 10,000 population) in the supply side (i.e.,
475 province i supplies food to other regions) and the M_C rate (deaths per 10,000 population) in the
476 demand side (i.e., province i receives food from other provinces) for a given province i .

477 The ΔM rates represent the level of balance between the M_P and M_C rates with the food system.
478 When the mortality rates from regional food production and consumption are balanced, ΔM equals
479 zero. If ΔM^i is >0 for a specific province, it indicates that the region experiences an excess number
480 of deaths owing to its food supply to other regions. These provinces are referred to as “production-
481 oriented,” while provinces with lower health damage ($M_C > M_P$) are labeled as “consumption-
482 oriented.”

483 Next, we ranked all the ΔM rates in ascending order and paired them with population data from

484 each region, following which the SDHII was computed using Eq. (12):

$$485 \quad SDHII = \frac{\sum_{i=1}^n POP_i \times |M_P^i - M_C^i|}{M} \quad (12),$$

486 where M and POP_i represent the national mortality rates and population for a given province i ,
487 respectively, and n denotes the total number of provinces.

488 Intuitively, SDHII corresponds to the area depicted in Fig. S3. This index represents the level of
489 national-scale inequality in health damage. It incorporates population proportion as a weighting
490 factor and captures the regional disparities arising from food production and consumption. When
491 the health damage experienced by a particular region aligns with the expected damage based on
492 food consumption, the ΔM rates for that region are zero, indicating no contribution to SDHII. In an
493 ideal scenario, each region bears health damage proportionate to its consumption, resulting in a
494 balanced distribution of premature mortalities and an SDHII value of 0.

495 To trace the transfer of health damage across different income groups, we divided all the provinces
496 into 10 income groups (labeled from D1 to D10 in the ascending order of income). Next, we
497 conducted pairwise matching among the income groups and calculated the difference in health
498 damage resulting from reciprocal food supply between them, enabling us to evaluate the net
499 premature mortality caused by the intergroup food supply, which is denoted as net ΔM , and can
500 be expressed by:

$$501 \quad \text{net } \Delta M^{i,j} = \Delta M^{i,j} - \Delta M^{j,i} \quad (13),$$

502 where net $\Delta M^{i,j}$ represents the net premature mortality between the selected income group i and
503 another given income group j . This metric evaluates the net health damage between the different
504 income groups after offsetting the respective health damage associated with food consumption. If
505 net $\Delta M^{i,j}$ is >0 , the income group j causes excess health damage to the income group i and gains
506 health benefits from food trade owing to the food supply from i to j . Conversely, if net $\Delta M^{i,j}$ is <0 ,
507 the group j experiences more health damage because of the food supply to the group i .

508 **Intervention strategies**

509 We investigated the potential cobenefits of reducing inequality from various intervention
510 approaches aimed at reducing emission or developing a balanced diet. We designed three
511 intervention scenarios: agricultural emission mitigation, diet transition, and agricultural production
512 reallocation. Each scenario includes several subscenarios that differ in implementation intensity,

513 feasibility, and expected benefits (Table S4).

514 We conducted five subscenarios to mitigate agricultural ammonia emissions, comprising three
515 single and two collaborative measures, as outlined by Adalibieke et al.²⁸. In the “Increasing
516 mechanized deep fertilization” (FDP) scenario, the incorporation proportion of synthetic N
517 fertilizers is set to reach 80% for wheat, maize, and rice based on the National Agriculture
518 Mechanization Extension Plan³⁷. In the “Optimizing fertilizer types” (FTP) scenario, we assumed
519 that 50% of N applications were allocated to organic fertilizer and manure for major crops,
520 vegetables, and fruits³⁷. In the “Optimizing fertilizer rates” (OFR) scenario, the N fertilizer rate was
521 reduced to meet the “N Surplus Benchmarks” in seven regions, as proposed by Zhang et al.³⁸ and
522 the European Union Nitrogen Expert Panel³⁹. The regional “N Surplus Benchmarks” were utilized
523 as the targeted N surplus in regions where the N surplus exceeds the benchmarks.

524 For the diet transition scenario, we explored the potential for reducing inequality by adopting
525 healthier dietary habits. Our dietary recommendations were based on the 2022 Chinese Dietary
526 Guidelines (CDG 2022). The scenario considered nine food categories: grain, vegetables, fruits, pig,
527 beef, sheep and goat, poultry, dairy, and eggs. Using CDG 2022 as a reference, we designed four
528 subscenarios for the entire population, balancing healthfulness and feasibility to varying degrees.
529 The four subscenarios included (1) adjusting food intake for each category to the upper limit of the
530 recommended range in CDG (Max); (2) adjusting food intake for each category to the lower limit
531 of the recommended range in CDG (Min); (3) adjusting food intake for each category to the average
532 values of the recommended range in CDG (Ave); and (4) adjusting food intake for each category
533 based on the minimum difference between the existing diet and the recommended range (Maint).
534 For example, if the current food intake exceeded the upper limit of the recommended range, it was
535 adjusted to the upper limit range. Conversely, if the intake was below the lower limit, it was
536 adjusted to the lower limit. No adjustments are made if the current intake is already within the
537 recommended range. We computed the percentage of changes in food intake owing to the dietary
538 transition of each food category, which formed the diet transition matrix (labeled as H_3), based on
539 which we recalculated the premature mortality for each food category in each province to
540 represent the changes in health damage and equality for each subscenario.

541 Agricultural production reallocation aimed to mitigate health damage by redistributing crop
542 production from high- to low-sensitivity areas. Certain regions are more susceptible to $PM_{2.5}$

543 emission, leading to more premature deaths per production unit than other regions. Herein, we
544 assumed a fixed spatial distribution of farmlands to avoid potential environmental footprints
545 related to alterations in land use, such as new farmland cultivation^{7,40}. Thus, we analyzed crop
546 reallocation by transferring production from farmlands with high PM_{2.5} sensitivity to existing
547 farmlands with PM_{2.5} sensitivity while maintaining crop yield. This transfer of crop yield from high-
548 to low-sensitivity areas requires a certain level of yield increase in those low-sensitivity regions.
549 While concentrating crop production in the areas with the lowest sensitivity would ideally
550 maximize health benefits, it is impractical owing to the limited production potential. We assumed
551 a 30% yield increase in each crop production area and a maximum reduction of 20% in the total
552 crop production in high-sensitivity areas considering the yield ceiling in low-sensitivity areas.
553 Consequently, we designed 20 subscenarios to transfer production from regions with higher
554 mortality rates per unit production (1%–20% of the total production) to regions with lower
555 mortality rates. First, we calculated the mortality rate per unit of crop production for each province
556 using data from the Chinese National Bureau of Statistics⁵. Then, starting with the province with
557 the highest mortality rates (province A), we transferred crop yield to the province with the lowest
558 mortality rates (province B) until the yield increase in province B reached 30% of its initial crop
559 yield. This process was repeated for the second-best province and continued until the total
560 transferred production yield reached 20%. We achieved the desired reallocation by sequentially
561 allocating transferred yields to regions with the lowest mortality rates per unit.

562 **Limitations**

563 Several limitations need to be acknowledged. The impact of national food imports and exports was
564 not considered due to a lack of data. Additionally, the results of this study are exclusively based on
565 data from 2017. Besides, the implementation of intervention scenarios could have profound
566 impacts on the economy, leading to changes in emissions and associated environmental impacts,
567 which are not considered in this study. Future work could expand the study period to encompass
568 multiple years, which would help to clarify the historical patterns and drivers of inequality.

569

570 **Acknowledgements**

571 This research is supported by the National Natural Science Foundation of China (42192511), the
572 Shenzhen Key Laboratory of Precision Measurement and Early Warning Technology for Urban
573 Environmental Health Risks (ZDSYS20220606100604008), Shenzhen Science and Technology
574 Program (JCYJ20220818100611024), the National Natural Science Foundation of China (41991312,
575 41821005, 41922057, and 41830641), Department of Science and Technology of Guangdong
576 Province (2021B1212050024), Department of Education of Guangdong Province (2021KCXTD004),
577 Energy Foundation (G-2111-33575), and Center for Computational Science and Engineering at
578 Southern University of Science and Technology.

579

580 **Author contributions**

581 H.S., J.M., P.H., and F.Z. conceived and initiated the study. L.Z. and W.A. processed and analyzed
582 the data. Y.C., P.G., J.H., and Y.Z. provided support with data collection and processing. P.X., C.W.,
583 J.Y., and L.Z. assisted in the development of the model framework. L.Z. drafted the manuscript, and
584 G.S., T.-M. F., and X.Y. participated in the result discussions. H.S., F.Z., J.M., P.H., S.Z., A.H., S.T., and
585 A.G.R. provided critical revisions.

586

587 **References**

- 588 1. Rudel, T. K. et al. Agricultural intensification and changes in cultivated areas, 1970–2005.
589 *Proceedings of the National Academy of Sciences* **106**, 20675-20680 (2009).
- 590 2. Bentham, J. et al. Multidimensional characterization of global food supply from 1961 to 2013. *Nature*
591 *Food* **1**, 70-75 (2020).
- 592 3. Kinnunen, P. et al. Local food crop production can fulfil demand for less than one-third of the
593 population. *Nature Food* **1**, 229-237 (2020).
- 594 4. Huang, X. et al. A high-resolution ammonia emission inventory in China. *Global Biogeochemical*
595 *Cycles* **26** (2012).
- 596 5. NBS. *China Statistical Yearbook 2017* (China Statistics Press, 2018).
- 597 6. Tessum, C. W. et al. Inequity in consumption of goods and services adds to racial–ethnic disparities
598 in air pollution exposure. *Proceedings of the National Academy of Sciences* **116**, 6001-6006 (2019).
- 599 7. Foley, J. A. et al. Solutions for a cultivated planet. *Nature* **478**, 337-342 (2011).
- 600 8. Chen, X. et al. Producing more grain with lower environmental costs. *Nature* **514**, 486-489 (2014).
- 601 9. Springmann, M. et al. Options for keeping the food system within environmental limits. *Nature* **562**,
602 519-525 (2018).
- 603 10. Gu, B. et al. Cost-effective mitigation of nitrogen pollution from global croplands. *Nature* **613**, 77-84
604 (2023).
- 605 11. Godfray, H. C. J. et al. Meat consumption, health, and the environment. *Science* **361**, eaam5324
606 (2018).
- 607 12. Poore, J. & Nemecek, T. Reducing food’s environmental impacts through producers and consumers.
608 *Science* **360**, 987-992 (2018).
- 609 13. Hasegawa, T., Havlík, P., Frank, S., Palazzo, A. & Valin, H. Tackling food consumption inequality to
610 fight hunger without pressuring the environment. *Nature Sustainability* **2**, 826-833 (2019).
- 611 14. Clark, M. et al. Estimating the environmental impacts of 57,000 food products. *Proceedings of the*
612 *National Academy of Sciences* **119**, e2120584119 (2022).
- 613 15. Halpern, B. S. et al. The environmental footprint of global food production. *Nature Sustainability* **5**,
614 1027-1039 (2022).
- 615 16. Lam, H.-M., Remais, J., Fung, M.-C., Xu, L. & Sun, S. S.-M. Food supply and food safety issues in China.
616 *The Lancet* **381**, 2044-2053 (2013).
- 617 17. He, P., Baiocchi, G., Hubacek, K., Feng, K. & Yu, Y. The environmental impacts of rapidly changing
618 diets and their nutritional quality in China. *Nature Sustainability* **1**, 122-127 (2018).
- 619 18. Zhao, S. et al. A multiphase CMAQ version 5.0 adjoint. *Geoscientific Model Development* **13**, 2925-
620 2944 (2020).
- 621 19. Sans, P. & Combris, P. World meat consumption patterns: An overview of the last fifty years (1961–
622 2011). *Meat Science* **109**, 106-111 (2015).
- 623 20. Bell, W., Lividini, K. & Masters, W. A. Global dietary convergence from 1970 to 2010 altered inequality
624 in agriculture, nutrition and health. *Nature Food* **2**, 156-165 (2021).
- 625 21. Ma, L., Long, H., Tu, S., Zhang, Y. & Zheng, Y. Farmland transition in China and its policy implications.
626 *Land Use Policy* **92**, 104470 (2020).
- 627 22. Xue, L. et al. China’s food loss and waste embodies increasing environmental impacts. *Nature Food*
628 **2**, 519-528 (2021).
- 629 23. *UN Sustainable Development Goals. Goal 10: Reduce inequality within and among countries.* (UN

- 630 Sustainable development group, 2022); <https://www.un.org/sustainabledevelopment/inequality/>
- 631 24. Zhai, F. et al. Prospective study on nutrition transition in China. *Nutrition reviews* **67**, S56-S61 (2009).
- 632 25. Zheng, H. et al. Chinese provincial multi-regional input-output database for 2012, 2015, and 2017.
- 633 *Scientific Data* **8**, 244 (2021).
- 634 26. Burnett, R. et al. Global estimates of mortality associated with long-term exposure to outdoor fine
- 635 particulate matter. *Proceedings of the National Academy of Sciences* **115**, 9592-9597 (2018).
- 636 27. Huang, Y. et al. Quantification of global primary emissions of PM_{2.5}, PM₁₀, and TSP from combustion
- 637 and industrial process sources. *Environmental Science & Technology* **48**, 13834-13843 (2014).
- 638 28. Adalibieke, W. et al. Decoupling between ammonia emission and crop production in China due to
- 639 policy interventions. *Global Change Biology* **27**, 5877-5888 (2021).
- 640 29. Wang, C. et al. A high-resolution ammonia emission inventory for cropland and livestock production
- 641 in China. *Chinese Journal of Eco-Agriculture* **29**, 1973-1980 (2021).
- 642 30. NBS. *China energy statistical yearbook 2017*. (China Statistics Press, 2017).
- 643 31. Zhao, H. et al. Assessment of China's virtual air pollution transport embodied in trade by using a
- 644 consumption-based emission inventory. *Atmospheric Chemistry and Physics* **15**, 5443-5456 (2015).
- 645 32. Shen, H. et al. Novel method for ozone isopleth construction and diagnosis for the ozone control
- 646 strategy of Chinese cities. *Environmental Science & Technology* **55**, 15625-15636 (2021).
- 647 33. Zhou, M. et al. Mortality, morbidity, and risk factors in China and its provinces, 1990-2017: a
- 648 systematic analysis for the Global Burden of Disease Study 2017. *The Lancet* **394**, 1145-1158 (2019).
- 649 34. Wang, X. et al. Sensitivities of ozone air pollution in the Beijing-Tianjin-Hebei area to local and
- 650 upwind precursor emissions using adjoint modeling. *Environmental Science & Technology* **55**, 5752-
- 651 5762 (2021).
- 652 35. Pappin, A. J. & Hakami, A. Source attribution of health benefits from air pollution abatement in
- 653 Canada and the United States: an adjoint sensitivity analysis. *Environmental Health Perspectives* **121**,
- 654 572-579 (2013).
- 655 36. Wang, M., Yim, S. H., Dong, G., Ho, K. & Wong, D. Mapping ozone source-receptor relationship and
- 656 apportioning the health impact in the Pearl River Delta region using adjoint sensitivity analysis.
- 657 *Atmospheric Environment* **222**, 117026 (2020).
- 658 37. Zhang, X. et al. Societal benefits of halving agricultural ammonia emissions in China far exceed the
- 659 abatement costs. *Nature Communications* **11**, 4357 (2020).
- 660 38. Zhang, C., Ju, X., Powlson, D., Oenema, O. & Smith, P. Nitrogen surplus benchmarks for controlling N
- 661 pollution in the main cropping systems of China. *Environmental Science & Technology* **53**, 6678-6687
- 662 (2019).
- 663 39. Panel, E. N. E. Nitrogen use efficiency (NUE): an indicator for the utilization of nitrogen in food
- 664 systems. *Wageningen University, Alterra, Wageningen, Netherlands* (2015).
- 665 40. Hong, C. et al. Global and regional drivers of land-use emissions in 1961-2017. *Nature* **589**, 554-561
- 666 (2021).